The intracellular uptake of CD95 modified paclitaxel-loaded poly(lactic-co-glycolic acid) microparticles

Davidson D. Ateh [a],[*], Veronica H. Leinster [a], Sally R. Lambert [a], Afsha Shah [a], Ayub Khan [a], Hazel J. Walklin [a], Jennifer V. Johnstone [a], Nader I. Ibrahim [a], Mustafa M. Kadam [a], Zain Malik [a], Míriam Gironès [b], Gert J. Veldhuis [b], Gary Warnes [c], Silvia Marino [d], Iain A. McNeish [e], Joanne E. Martin [a]

[a] Pathology Group, Blizard Institute, Barts and The London School of Medicine and Dentistry, Queen Mary, University of London, 4 Newark Street, London E1 2AT, UK
[b] Nanomi BV, Zutphenstraat 51, 7575 EJ Oldenzaal, The Netherlands
[c] Flow Cytometry Core Facility, Blizard Institute, Barts and The London School of Medicine and Dentistry, Queen Mary, University of London, 4 Newark Street, London E1 2AT, UK
[d] Neuroscience & Trauma, Blizard Institute, Barts and The London School of Medicine and Dentistry, Queen Mary, University of London, 4 Newark Street, London E1 2AT, UK
[e] Centre for Molecular Oncology & Imaging, Barts Cancer Institute, Barts and The London School of Medicine and Dentistry, Queen Mary, University of London, Charterhouse Square, London EC1M 6BQ, UK

ARTICLE INFO

ABSTRACT

The CD95/CD95L receptor-ligand system is mainly recognised in the induction of apoptosis. However, it has also been shown that CD95L is over-expressed in many cancer types where it modulates immune-evasion and together with its receptor CD95 promotes tumour growth. Here, we show that CD95 surface modification of relatively large microparticles >0.5 μm in diameter, including those made from biodegradable polylactic-co-glycolic acid (PLGA), enhances intracellular uptake by a range of CD95L expressing cells in a process akin to phagocytosis. Using this approach we describe the intracellular uptake of microparticles and agent delivery in neurons, medulloblastoma, breast and ovarian cancer cells in vitro. CD95 modified paclitaxel-loaded PLGA microparticles are shown to be significantly more effective compared to conventional paclitaxel therapy (Taxol) at the same dose in subcutaneous medulloblastoma (***$P < 0.0001$) and orthotopic ovarian cancer xenograft models where a >65-fold reduction in tumour bioluminescence was measured after treatment (*$P = 0.012$). This drug delivery platform represents a new way of manipulating the normally advantageous tumour CD95L over-expression towards a therapeutic strategy. CD95 functionalised drug carriers could contribute to the improved function of cytotoxics in cancer, potentially increasing drug targeting and efficacy whilst reducing toxicity.

1. Introduction

Intracellular drug candidates have advanced beyond serendipitous discoveries towards small molecules, peptides, proteins and nucleic acids with predefined targets. However, delivery to the interior of cells remains problematic and active compounds often fail to be developed into drugs. In a related issue, the effectiveness of cytotoxic drug administration in cancer is limited by systemic drug clearance and off-target toxicity. We report the use of the CD95 receptor (also called Fas and Apo-1) in the surface modification of drug-loaded microparticles to enhance targeted intracellular drug delivery. CD95 is mainly recognised as a promoter of apoptosis after binding with its ligand CD95L, of the TNF super-family. CD95/CD95L has been mostly studied for this effect [1] and deregulation of the system is associated with breakdown in immune homeostasis [2]. The BioGPS database reports that high CD95 gene expression in normal tissue is associated with immune cells such as B lymphoblasts and CD4+ T cells [3] whilst CD95L gene expression is prominent in CD56+ NK cells [4].

Beyond a singular role in immune tissues, there are reports suggesting important functions for the CD95/CD95L system in immune privileged tissues such as the central nervous system, where CD95 and CD95L are expressed by non-immune cells [5]. This includes novel roles in Parkinson's [6] and Alzheimer's [7] diseases as well as spinal cord injury [8]. Furthermore, there is strong evidence that the expression of CD95L in tumours [9–11] confers immune privileged status by enabling the killing of activated CD95-positive immunocytes [12]. Tumour cells expressing

* Corresponding author. Tel.: +44 20 7882 2286; fax: +44 20 7882 2180.
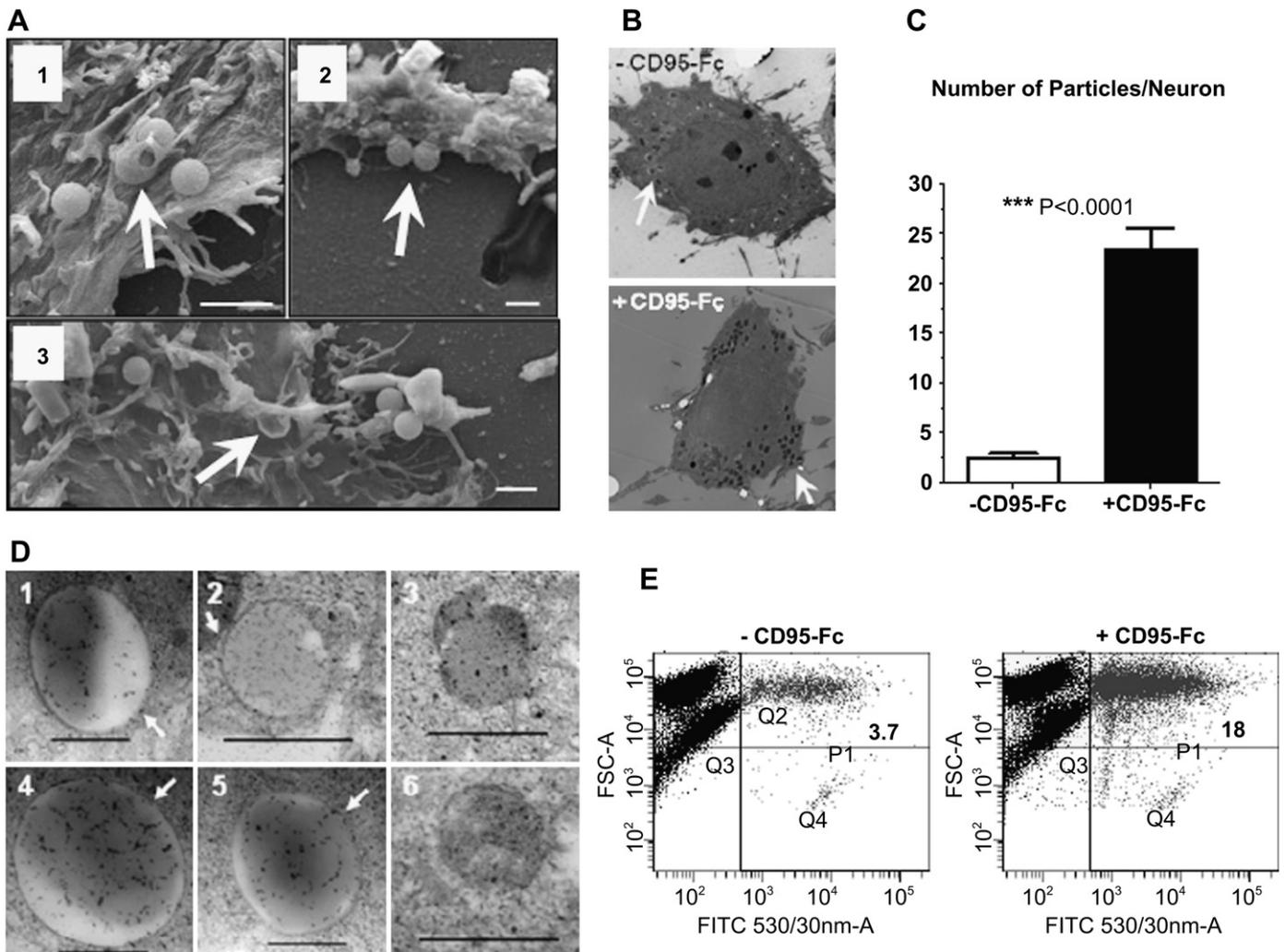E-mail address: d.d.ateh@qmul.ac.uk (D.D. Ateh).

Fig. 1. Electron microscopy and FACS confirm that CD95 modification enhances the intracellular uptake of microparticles by sensory neurons in vitro. (A), Scanning electron microscopy shows the dynamic interaction of primary DRG neurons with particles at the cell membrane. The arrows show examples of (1) the neuronal membrane enveloping a microparticle, (2) projections from the neuronal membrane around the base of two microparticles and (3) a phagocytic cup where a microparticle may have been dislodged. Scale bar, 1 μm (B), Transmission electron microscopy shows cross-sections of DRG neurons challenged with control and CD95-Fc coated polystyrene microparticles. These generally appeared as well formed dark spheres (white arrows) and uptake was noted for both −CD95-Fc and +CD95-Fc microparticles. (C), Uptake of CD95-Fc coated microparticles was significantly higher upon quantification with up to 67 +CD95-Fc microparticles found in a single cell compared to a maximum of 15 for uncoated microparticles. ****$P < 0.0001$. Values represent mean ± SEM, $n = 50$. (D), Microparticles were predominantly found enclosed in a double membrane (white arrows) reminiscent of phagosomes but there were a few examples of microparticles without double membranes (3,6), presumably degraded during intracellular trafficking. Scale bar, 0.5 μm (E), Flow cytometry confirmed enhanced uptake for +CD95-Fc microparticles in the ND7/23 sensory neuron cell line.

CD95L include glioblastoma [13] and medulloblastoma [14] brain tumours as well as ovarian cancers [15] where there is significantly increased CD95L expression in malignant ovarian tumours compared to benign tumours [16,17]. There is also recent and compelling data suggesting an alternative role for the CD95/CD95L system as tumour growth promoter [18,19] rather than suppressor.

Targeted delivery of therapeutic nanoparticles to diseased cells is a common strategy [20] whilst the use of larger microparticles (>0.5 μm) is focussed primarily on immune cells known to be phagocytic. However, many cell types, often termed non-professional phagocytes [21] have the capacity to ingest relatively large microparticles and this must be modulated by as yet poorly understood cell membrane signals [22]; for example, telencephalin was shown to modulate the phagocytic uptake of microparticles in the specific case of hippocampal neurons [23,24]. We studied cell surface ligands including those not known to be involved in phagocytosis and noted enhanced uptake of CD95 microspheres by challenged CD95L expressing cells. This paper describes the CD95 enhanced phagocytic uptake of microparticles and an important application in targeted

chemotoxin drug delivery, with the potential for enhanced efficacy and decreased systemic toxicity.

2. Materials and methods

2.1. PLGA biodegradable microparticle synthesis

2.1.1. Double emulsion method
Ethidium homodimer (Eth-D) (Sigma, UK) loaded polylactic-co-glycolic acid (PLGA) (RG502H, Boehringer Ingelheim, Germany) biodegradable microspheres were prepared by double emulsion as previously described [25]. Briefly, an organic phase consisting of PLGA in dichloromethane with ethidium homodimer dye was vigorously agitated under probe sonication to form a primary emulsion. This was added to a 4% polyvinyl acid aqueous solution and further agitated to form a secondary emulsion. Microspheres were collected by centrifugation after removal of organic solvent in the evaporation phase. Eth-D PLGA microparticles were polydisperse and were post-filtered through 1.2 μm polycarbonate filters (Millipore, UK).

2.1.2. Microsieve emulsification
PLGA (RG502H, Boehringer Ingelheim, Germany) placebo (unloaded) microspheres were prepared by a single emulsion solvent evaporation technique, microsieve emulsification. Prior to emulsification a 7% w/v PLGA solution in
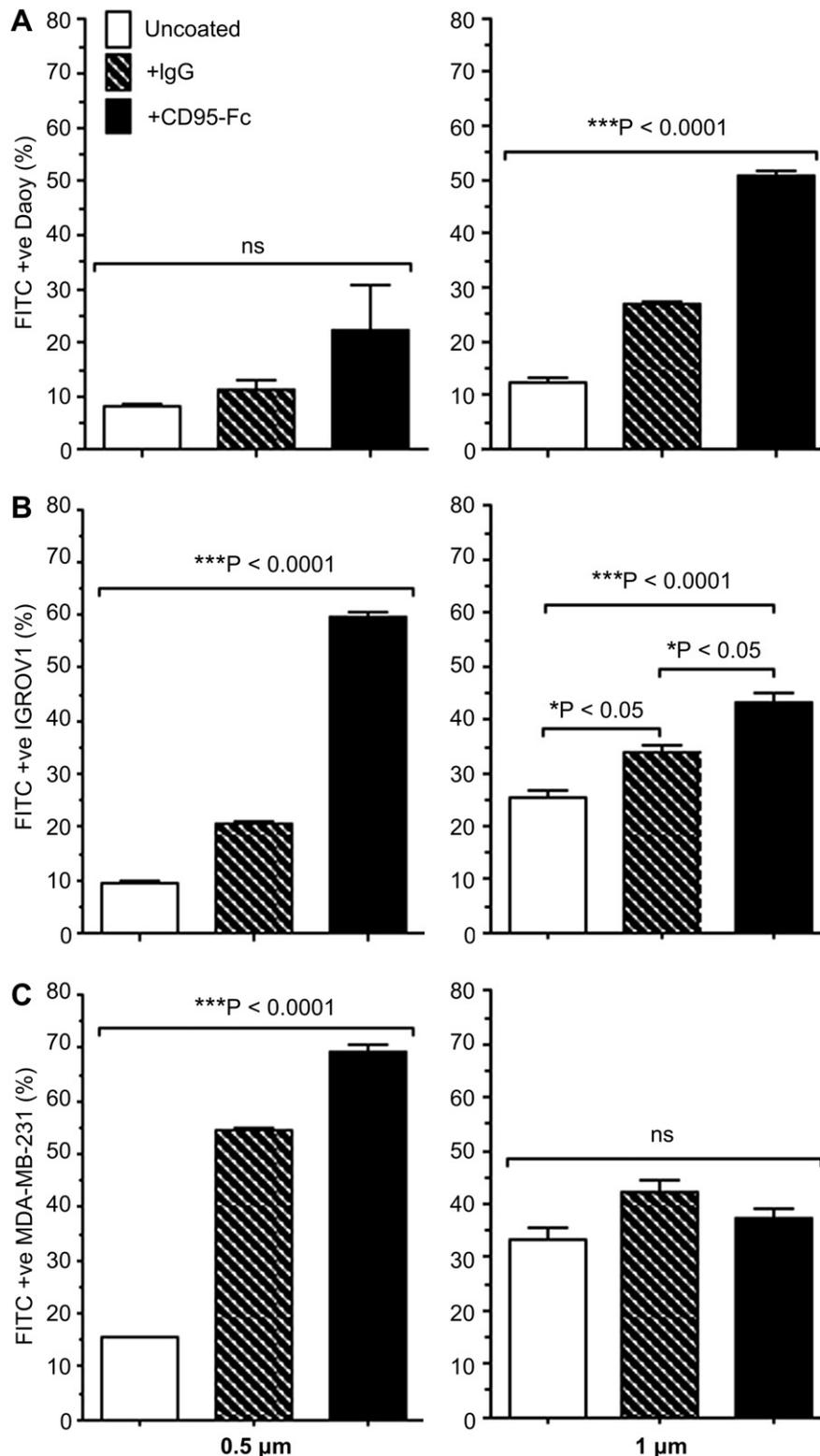
Fig. 2. FACS confirms that CD95 modification enhances the intracellular uptake of microparticles by cancer cells. (A), Human Daoy (medulloblastoma) cells. (B), Human IGROV1 (ovarian cancer) cell line. (C), Human MDA-MB-231 (breast cancer) cell line. Mean ± SEM, $n = 3$ (percentage of particle uptake summarised from 3 independent FACS experiments ≥ 10,000 events).

dichloromethane was filtered through a 0.2 μm PTFE filter. Thereafter the PLGA was emulsified through a microsieve membrane (Nanomi BV, The Netherlands), which is a microfabricated membrane with uniform pores along the surface, into an aqueous solution containing an emulsifier. The resultant emulsion was left to stir at room temperature for at least 3 h to evaporate the solvent. The hardened microspheres were concentrated by filtration and washed repeatedly. Subsequently, the particles were freeze-dried and stored at −20 °C until evaluation. For paclitaxel-loaded PLGA (RG502H, Boehringer Ingelheim, Germany) microspheres, paclitaxel was added and dissolved into a 6% w/v PLGA solution in dichloromethane in order to achieve a final microparticle drug concentration of 25% w/w. The solution was filtered through a 0.2 μm PTFE filter and emulsified through a silicon microsieve. Ultrapure water containing an emulsifier was used as continuous phase. The emulsion was
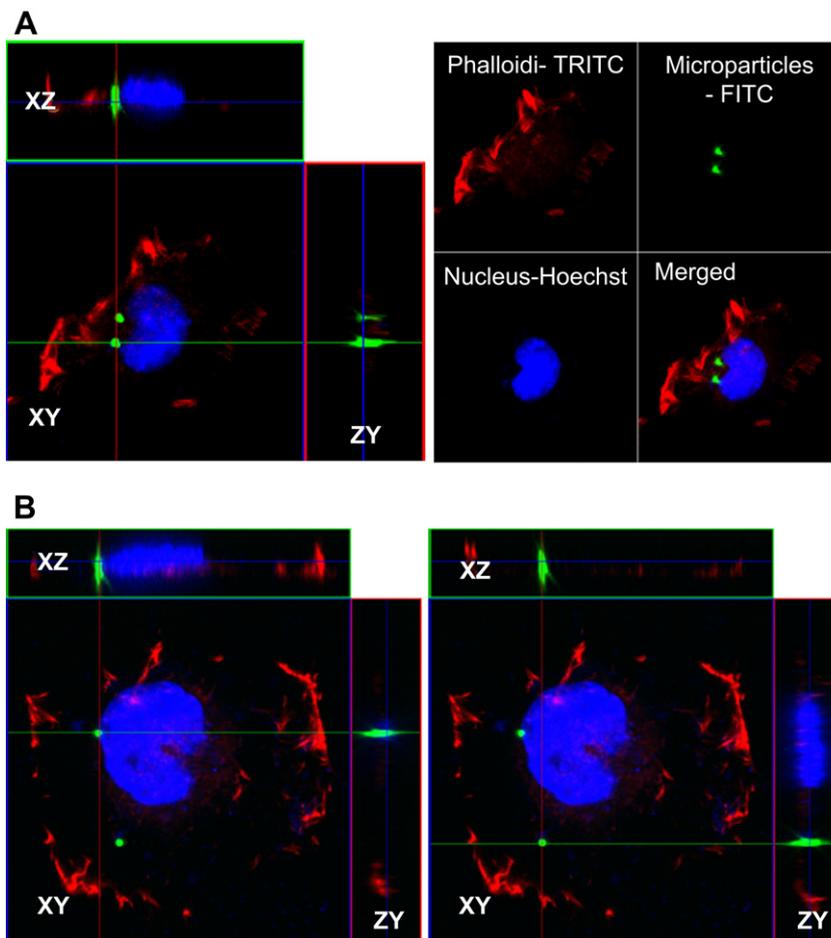
Fig. 3. Confocal microscopy confirms internalisation of inert 1 μm microparticles by Daoy medulloblastoma cells. (A), This first example shows the uptake of two microparticles by Daoy cells. Separated channels and merged data for confocal image shown on left. Actin cytoskeleton stained red and nucleus blue. (B), Another confocal image example showing a Daoy cell with two internalised particles. Both particles can be seen within the cytoplasm on the Z-sections (XZ & ZY) co-localising with the actin stain. ×63 objective magnification. (For interpretation of the references to colour in this figure legend, the reader is referred to the web version of this article.)

magnetically stirred for at least 3 h at room temperature to evaporate dichloromethane. After solidification microspheres were also collected by filtration and washed repeatedly. Subsequently, the particles were freeze-dried and stored at −20 °C until evaluation. Particles were characterised in terms of particle size distribution by optical microscopy, Coulter Multisizer (Beckman Coulter), CPS centrifuge sizer and SEM.

2.2. Microparticle surface modification

For experiments, polystyrene or PLGA microparticles were either sham coated in phosphate buffer saline (PBS) or coated by physical adsorption in 5 μg/100 μl PBS of respective protein (fibronectin, vitronectin, IgG [02-6502, Invitrogen, UK] and CD95-Fc [F8799, Sigma, UK]) for 90 min (vortexed every 30 min) to ensure adequate adsorption. Modified microparticles were then centrifuged and re-suspended in PBS for experimental use.

2.3. Microparticle internalisation assays (FACS)

Cultures seeded at 2×10^5 cells/60 mm dish were established for at least two days in low serum (2–5%) DMEM prior to challenge with fluorescent microparticles (uncoated and coated) at either 0.5 or 1 μm in diameter (FS03F/5069 & FS03F/7220, Bangs laboratories, USA). Fluorescent microparticles were incubated with cultures (10^5, 10^6 or 10^7) for 24 h prior to flow cytometry measurement (1 h for control experiments described in Supplementary Fig. 4B). Following incubation, non-internalised microparticles were removed by triple washes in Hanks. Adherent cells were trypsinised off the dish and transferred to centrifuge tubes. Cells were spun down at 1000 RPM for 5 min, supernatant was removed and cells were kept on ice re-suspended in Hanks after transfer to flow cytometry tubes. Cells were then analysed by flow cytometry (FACScan flow cytometer with Cellquest Pro software) for a minimum of 10,000 events. Multiple parameters were recorded including forward scatter, side scatter and fluorescent channels (FL1 recorded cells that ingested FITC positive fluorescent microparticles, FL2 recorded ethidium

homodimer-loaded PLGA microparticles). Supplementary Fig. 4A presents data analysis, briefly gating was set using appropriate controls and cells with internalised microparticles were quantified in the upper right quadrant of FACS histograms.

For blocking experiments, 200 ng/ml CD95-Fc (F8799, Sigma, UK) was applied for either 15 min or 4 h, media was then replaced prior to the addition of microparticles and subsequent analysis as described above.

2.4. Cell death assay (FACS)

Cell death after addition of direct paclitaxel, uncoated and coated paclitaxel-loaded PLGA microparticles as well as uncoated and coated placebo microparticles was measured by FACS after addition of the 7-AAD viability stain (10042-01, Southern Biotech, USA). Cultures seeded at 2×10^5 cells/60 mm dish were established at least two days prior to challenge with treatments. Treatments were added to cultures for 24 h at which point culture media was replenished and cells maintained for a further two days prior to viability analysis (Supplementary Fig. 9a also shows results for IGROV1 cells directly after 24 h treatment and 2, 5 & 7 days following treatment). Paclitaxel was tested at 0.1 μg-50μg/60 mm dish (suspended in 2 ml of culture media) with the dose matched in loaded PLGA microparticles. On measurement day, cells were collected without washing (to avoid losing dead cells) as described for internalisation assays. Prior to flow cytometry measurement, 10 μl 7-AAD was added to each tube for 20 min. Naïve cells not exposed to any treatment were used as controls and hydrogen peroxide (H_2O_2) pre-exposed cells (4 h) served as positive controls. 7-AAD penetrated dead cells and these were observed in the FL3 fluorescent channel (FACScan flow cytometer with Cellquest Pro software).

2.5. In vivo experiments

Experiments were carried out under suitable UK Home Office personal and project license authority.

2.5.1. Medulloblastoma subcutaneous xenograft

1×10^6 Daoy medulloblastoma cells suspended in matrigel were inoculated by subcutaneous injection into NOD/SCID mice on day 1. Paclitaxel (20 mg/kg) and PLGA microspheres (dose matched) doses were administered by two intratumoral injections on day 7. Tumour length and width were recorded every 2–3 days and tumour volumes were approximated from the formula width^2 × length/2.

2.5.2. Ovarian cancer intraperitoneal xenograft

5×10^6 IGROV1-luciferase cells were inoculated by intraperitoneal (IP) injection into female Balb C nu/nu mice on day 1. Paclitaxel (20 mg/kg) and PLGA microspheres (dose matched) were administered IP once per week (days 7, 14, 21 and 28). For bioluminescence imaging, mice were injected IP with 125 mg/kg D-luciferin (Calliper Life Sciences, UK) and then anesthetized (2% isofluorane by inhalation). Five minutes later, whilst still under anaesthetic, they were placed in a light-tight chamber on a warmed stage (37 °C) and light emission from a defined region of interest on a ventral surface was imaged on a Xenogen IVIS Imaging System 100 (Alameda, USA). Data were analysed using Living Image software (also Xenogen, Alameda, USA) and are presented as relative radiance and mean Radiance (photons/s/cm2/sr).

3. Results

3.1. Neuronal microparticle uptake

Microparticles are sporadically ingested by sensory and cortical neurons [22] and this can be modulated by cell surface receptors (Supplementary Fig. 1). To verify the effect of CD95 modification we surface coated polystyrene microparticles and studied sensory neuron uptake by electron microscopy and flow cytometry (Fig. 1). Scanning electron microscopy revealed an active process akin to phagocytosis characterised by primary sensory neuron plasma membrane extension and envelopment of microparticles (Fig. 1A). Examination under the transmission electron microscope showed that ingested microparticles were generally contained within double membranes reminiscent of phagosomes (Fig. 1B and D). Transmission electron microscopy showed no ultrastructural toxicity even for neurons that ingested large numbers of polystyrene microparticles for the time periods studied (up to 1 week). Neuronal particle uptake was quantified (Fig. 1C and Supplementary Fig. 2A) and superior uptake recorded for the CD95 modified microparticles compared to uncoated controls (−CD95-Fc). This effect was confirmed with the ND7/23 sensory neuron cell line in flow cytometry experiments (Supplementary Fig. 2B). These results suggest a role for cell surface expressed CD95L, the only known ligand for CD95, in the uptake of extracellular material by sensory neurons.

3.2. Cancer cell microparticle uptake

CD95L expression is up-regulated in a number of tumour types [19] and we challenged medulloblastoma, ovarian and breast cancer cell lines with unmodified and CD95 surface coated inert microparticles (Fig. 2 and Supplementary Fig. 3). IgG was used to control for the Fc portion of the soluble CD95-Fc fusion protein (only soluble commercial form available). In general, uptake of CD95 modified microparticles was superior and microparticle uptake was size and cell type dependent. Flow cytometry was used to measure the uptake of fluorescent microparticles and precautions were taken to eliminate the inclusion of non-internalised particles (Supplementary Fig. 4). Intracellular uptake of microparticles was further confirmed by confocal microscopy (Fig. 3). Increased uptake of CD95 modified microparticles could be knocked down by blocking cell surface CD95L by CD95-Fc pre-exposure (Fig. 4). We tested for cell death in Daoy medulloblastoma cells after exposure to inert microparticles and there was none at particle concentrations used here, whilst minimal increases were noted when concentrations were raised by an order of magnitude (data not shown). These results confirm unrecognised

functions for CD95/CD95L beyond induction of apoptosis, adding further weight to recent changes in thinking in relation to tumour biology [18,19]. It is difficult to ascertain CD95L expression in cells as there is asynchronous transcription and translation as well as cell dependent cyclic expression [26]. Nevertheless, cell types studied here were all immunoreactive to CD95L antibody (Supplementary Fig. 5), results confirmed in literature reports.

3.3. In vitro drug delivery

To test whether improved microparticle uptake could be translated into more efficient delivery of intracellular drugs we synthesised poly(lactic-co-glycolic acid) (PLGA) biodegradable microparticles (Fig. 5). In the first instance, ethidium homodimer (membrane impermeable nucleic acid dye) loaded PLGA microparticles were used to test intracellular release after biodegradable particle uptake. This was achieved in primary sensory neurons (Fig. 6A) where we observed intracellular release from CD95 modified particles. The staining pattern was consistent with ribosome (nucleic acid rich) cytoplasmic distribution; the dye did not co-localise with the cell nucleus indicating that the cell was viable and the intact nuclear membrane restricted dye access (ethidium homodimer only penetrates compromised cell membranes). The CD95 modification increased ethidium homodimer uptake by Daoy medulloblastoma cells nearly 10-fold compared to excess direct dye added to cultures (Fig. 6B). For drug studies, we used a new microsieve emulsification manufacturing method to produce uniformly sized paclitaxel-loaded and placebo microparticles (Fig. 5B–D).

Microsieve emulsification avoids the need for post-filtering, reducing wastage of valuable active ingredients and allowing tight control over desired particle size [27]. The well established paclitaxel chemotoxin was chosen as a model drug to incorporate due to its intracellular specificity, interfering with microtubule breakdown. CD95 modified PLGA paclitaxel-loaded microparticles were cytotoxic to Daoy medulloblastoma cells (Fig. 6C) after cell viability measurements by FACS using the 7-AAD viability dye. Cytotoxicity was superior to all groups tested for this cell type. These microparticles were effective in other cell types tested (Supplementary Fig. 6) with variations in response to treatment corresponding to dose or measurement day following treatment. For example, CD95 modified microparticles appeared to work quicker than other treatment groups for IGROV1 cells (Supplementary Fig. 6A). It must be noted that in these experiments, high placebo doses (matched to drug-loaded microparticles) were also cytotoxic due to PLGA
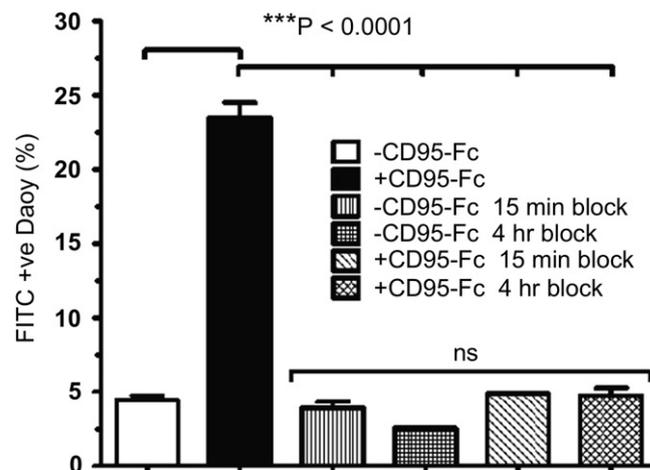

Fig. 4. Enhanced uptake of microparticles could be blocked by pre-exposure of Daoy cells to CD95-Fc prior to microparticle addition.
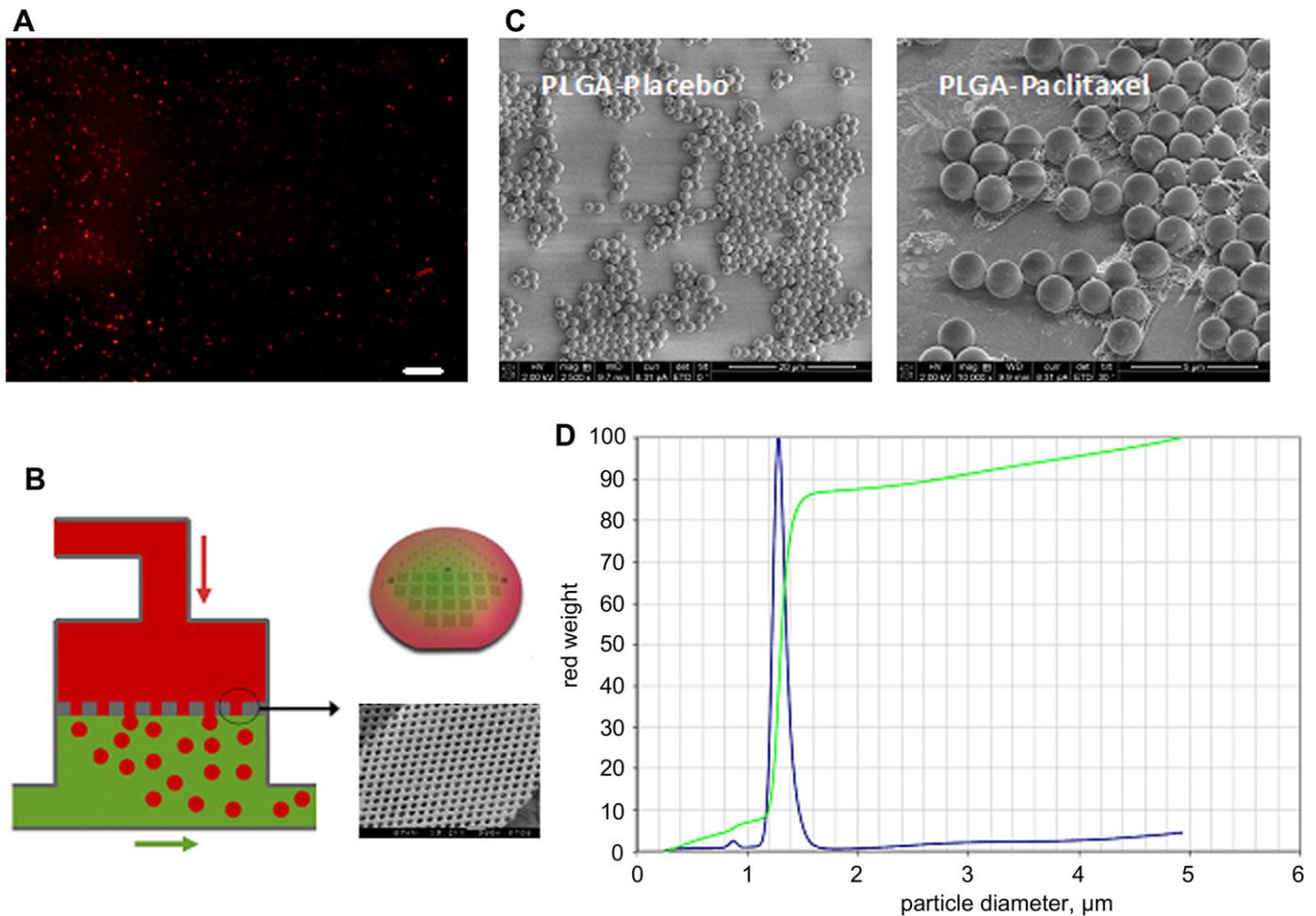
Fig. 5. Synthesis of poly(lactic-co-glycolic acid) (PLGA) biodegradable microparticles. (A), Ethidium homodimer (Eth-D) loaded PLGA microparticles (red) were synthesised by the well established double emulsion method under probe sonication agitation. This results in a polydisperse sample that was subsequently filtered to remove excessively large particles. Scale bar = 50 μm (B), The microsieve emulsification synthesis route is a novel process for the manufacture of uniformly sized microparticles with very low coefficient of variation (~5%). The fluid (red) is solvent dissolved PLGA and agent to be encapsulated which is emulsified through a silicon microsieve membrane with uniform pores. Right side images show a wafer containing microsieves (enlarged bottom right) fabricated by semiconductor technology. This new method removes the need for post-filtering. (C), Scanning electron microscopy images of monodisperse microparticles used in this study. Average diameters were measured as 1.6μm ± 0.18 (n = 60) for PLGA placebo (unloaded) microparticles and 1.4μm ± 0.07 (n = 51) for PLGA paclitaxel (25% w/w) microparticles. Mean ± sd. (D), Typical particle size distribution for PLGA paclitaxel microparticles batch as measured by CPS centrifuge sizer (coefficient of variance is 7.16%). (For interpretation of the references to colour in this figure legend, the reader is referred to the web version of this article).

breakdown products (glycolic and lactic acid). Furthermore, this assay could also report the effect of paclitaxel that may have leached from extracellular microparticles although precautions were taken to wash away non-internalised particles after 24 h exposure. The ability of CD95 modified microparticles to target drugs in an intact biological system with clearance mechanisms was therefore investigated in murine xenograft models.

3.4. In vivo drug delivery

We experimented in two different *in vivo* models. The first was a subcutaneous xenograft of Daoy medulloblastoma cells. This is an aggressively growing tumour and the study period was limited to two weeks after implantation. +CD95-Fc PLGA paclitaxel, +CD95-Fc placebo and unmodified (−CD95-Fc) paclitaxel microparticles all inhibited tumour growth to a greater extent than paclitaxel alone after a single intratumoural injection (Fig. 7A). There were no significant statistical differences between these three lowest volume change groups (Fig. 7B). In this model, the inhibitory effect of unmodified (−CD95-Fc) paclitaxel microparticles was likely to be due to better bioavailability than paclitaxel alone after

intratumoural injection, since the large microparticles (*ca* 1.5 μm) are retained within the tumour and locally release the cytotoxic. Interestingly, the inhibitory effect of CD95 modified placebo matched paclitaxel-loaded particles and was superior to unmodified (−CD95-Fc) placebo. This indicates active Daoy medulloblastoma cell targeting, enhanced intracellular uptake and prolonged cytotoxic effects for modified placebo particles, whereas cytotoxicity due to PLGA breakdown is only seen up to day four with unmodified particles. It is also possible that the CD95-Fc surface coating is interfering with CD95/CD95L mediated tumour proliferation as demonstrated in glioblastoma [18] and ovarian cancer [19]. However, since the applied CD95-Fc surface coating was a minute fraction of that reported for therapeutic phase II clinical trials (www.clinicaltrials.gov, APG101 in glioblastoma to inhibit migration) this is unlikely to be a significant contributor. Final masses for tumours collected in week three of the study were recorded (Supplementary Fig. 7A and B).

Moving to a more clinically relevant scenario, we used an orthotopic and established model of disseminated ovarian cancer [28] to target CD95L expressing IGROV1-luciferase cells within a compartmentalised space in the presence of other competing cell
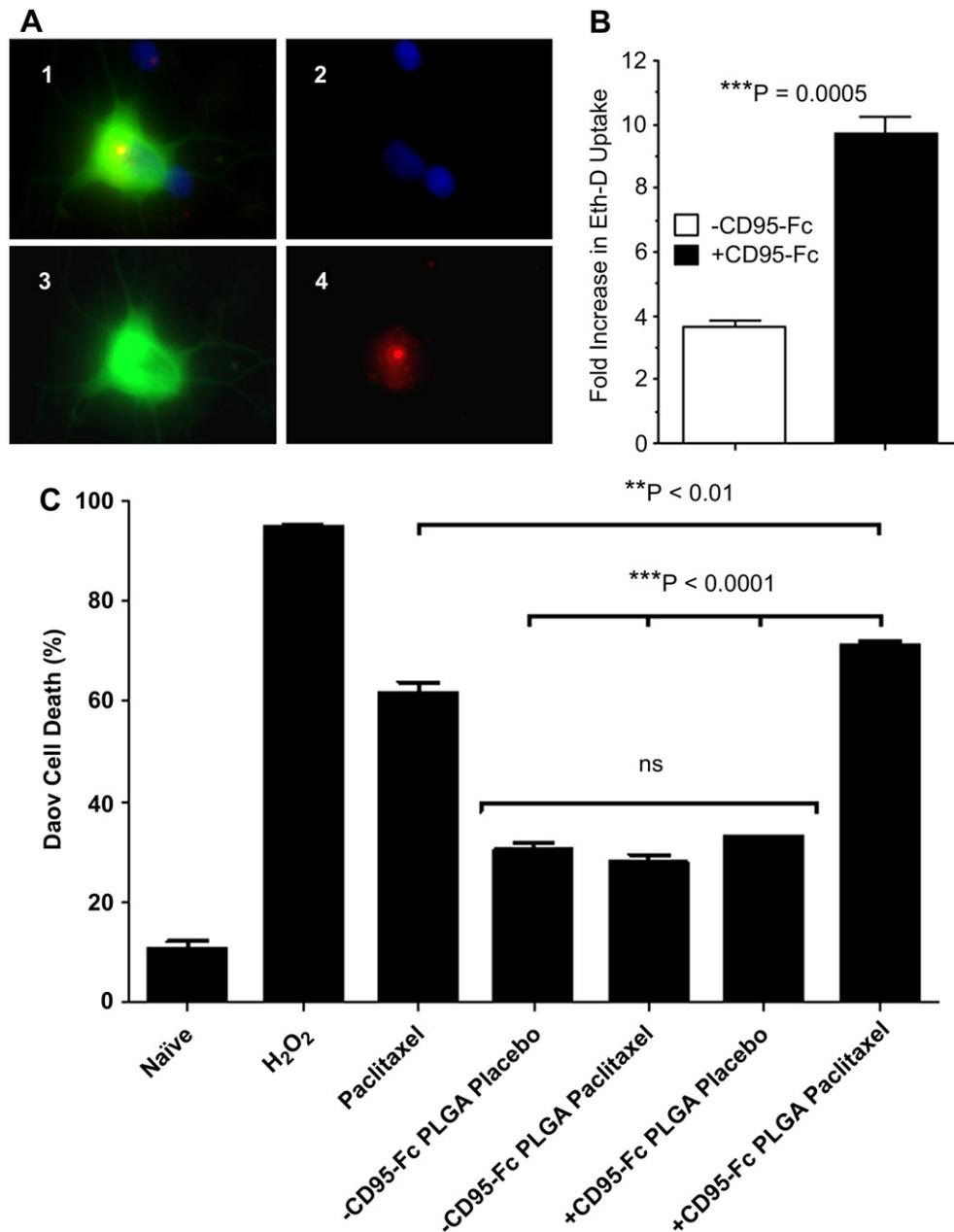
Fig. 6. CD95 modification enhances the intracellular uptake of biodegradable microparticles and delivery of agents to sensory neurons and cancer cells in vitro. (A), Ethidium homodimer delivery to sensory neurons. (1) Merged image. +CD95-Fc polylactic-co-glycolic acid biodegradable microparticles loaded with the ethidium homodimer dye (red) were taken up by primary DRG sensory neurons (green) in culture and delivered the dye to the cytoplasm. The ethidium homodimer small molecule is not capable of penetrating the membrane of viable cells without the microparticle carrier. (2) Nuclei in blue. (3) β3 tubulin neuronal marker in green. (4) Ethidium homodimer-loaded PLGA particle in red (<1.2 μm) with release of dye (after 48 h) and labelling of cytoplasmic nucleic acids. ×63 objective magnification. (B), Fold increase in ethidium homodimer (Eth-D) loaded microparticles uptake compared to naked dye for Daoy medulloblastoma cells. (C), CD95 modification enhances the biological efficacy of paclitaxel on Daoy cells at 2 days post-treatment. Mean ± SEM, $n = 3$ (summarised from 3 independent FACS experiments ≥ 10,000 events). (For interpretation of the references to colour in this figure legend, the reader is referred to the web version of this article.)

types (e.g. macrophages) by intraperitoneal injection (Fig. 8). Live imaging showed a >65-fold reduction in tumour bioluminescence by week 4 (Fig. 8A) for the +CD95-Fc PLGA paclitaxel treated group compared with an equivalent dose of Taxol, the clinical standard-of-care therapy (paclitaxel dissolved in Cremophor EL and ethanol). Unmodified (−CD95-Fc) PLGA paclitaxel matched Taxol. In this model, both placebo treatments (+CD95-Fc and −CD95-Fc) were ineffective, presumably due to less well focused cytotoxicity in the larger space compared with medulloblastoma intratumoural injections. The significant tumour reduction effect for +CD95-Fc PLGA paclitaxel treatment persisted after treatment suspension

(Fig. 8A and Supplementary Fig. 7C—E). Mice in this group all survived up to day 48 and at day 62 termination 80% asymptomatic animals remained (Supplementary Fig. 7E).

4. Discussion

The potential to inhibit tumour growth with taxane derivatives is well established in clinical use and since the original Taxol formulation (paclitaxel dissolved in Cremophor EL and ethanol) there have been succesful reformulations such as the Cremophor free Abraxane (paclitaxel bound to albumin nanoparticles)
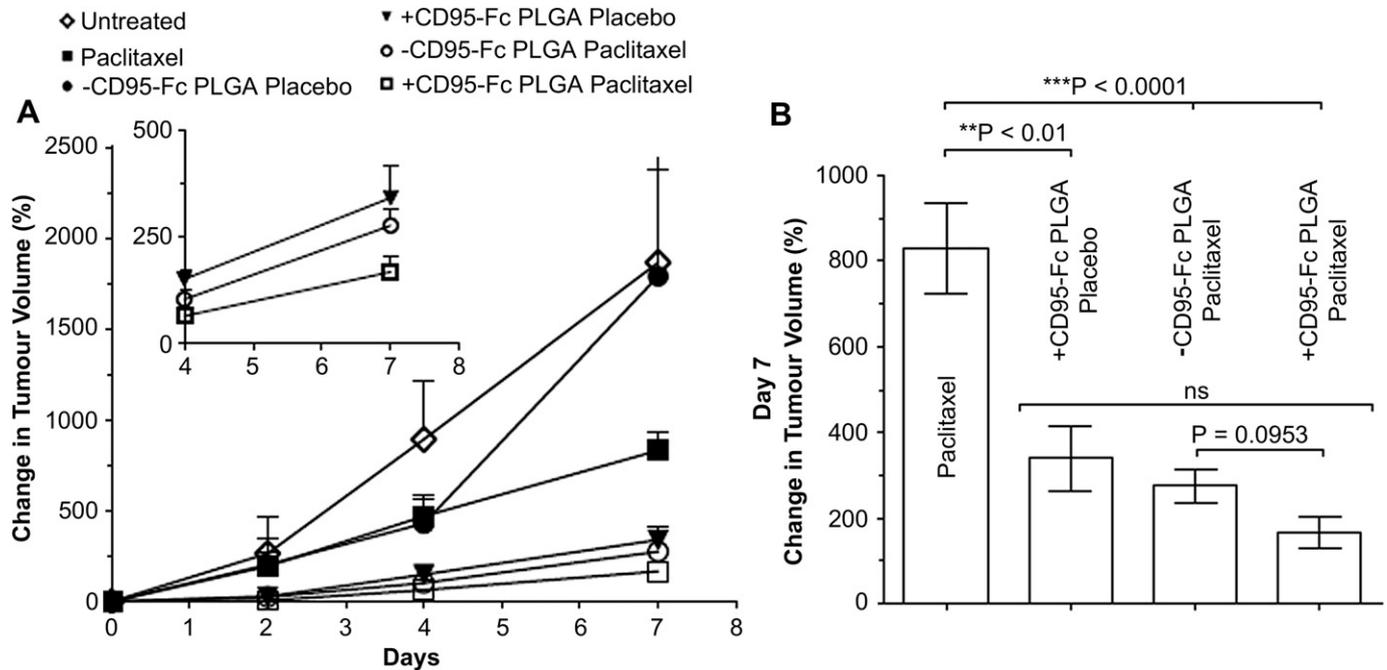
Fig. 7. CD95 modification enhances the efficacy of paclitaxel-loaded microparticles in a medulloblastoma subcutaneous xenograft. (A), Change in tumour volume is shown for an aggressively growing medulloblastoma subcutaneous xenograft. (B), On day 7 after single intratumoral injections, tumour growth was inhibited more efficiently for +CD95 PLGA placebo, −CD95 PLGA paclitaxel and +CD95 PLGA paclitaxel compared to paclitaxel alone. Mean ± SEM, $n = 4$.
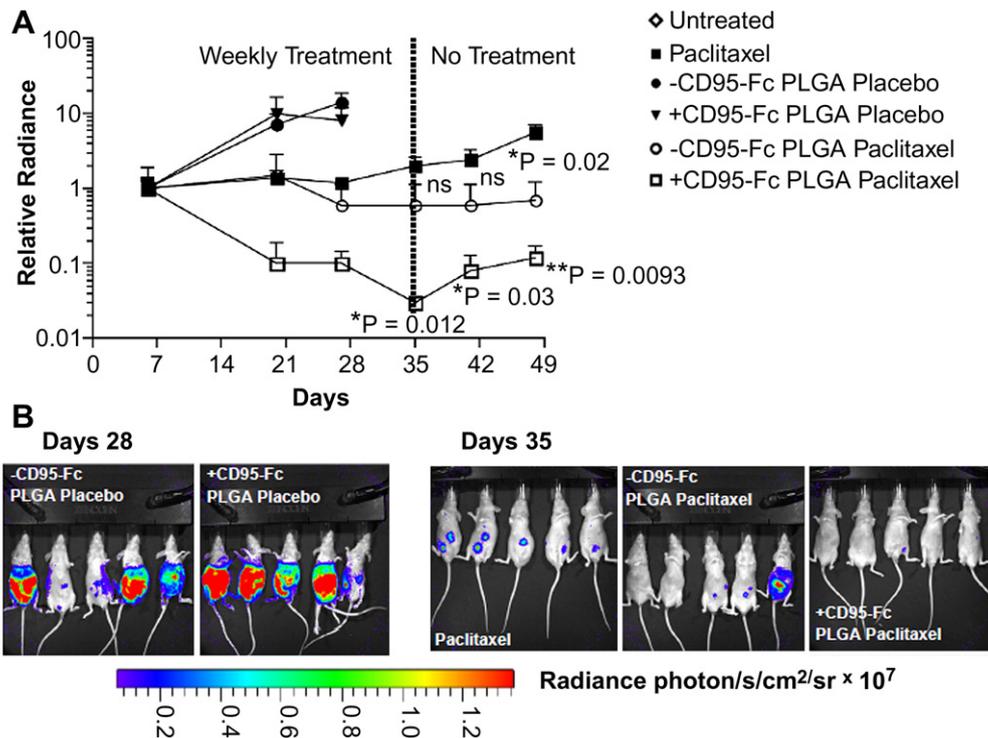

Fig. 8. CD95 modification enhances the efficacy of paclitaxel-loaded microparticles in an ovarian cancer orthotopic xenograft. (A), In a murine model of peritoneal ovarian cancer dissemination (IGROV1-luciferase expressing cancer cells), anti-tumour efficacy is shown for +CD95-Fc PLGA paclitaxel compared to an equivalent dose of paclitaxel formulated as Taxol after 4 weekly treatment administrations by a >65-fold difference in tumour bioluminescence. Mean ± SEM, $n = 5$. Tumour inhibition is maintained for the +CD95-Fc PLGA paclitaxel group after treatment suspension. Both placebo groups had to be sacrificed by day 28 due to extent of disease spread; by day 35, 1 animal in the −CD95-Fc PLGA paclitaxel group was sacrificed; by day 48, a further 2 animals in the −CD95-Fc PLGA paclitaxel, 2 in the paclitaxel and 1 in the +CD95-Fc PLGA paclitaxel group were sacrificed. Statistical comparisons are shown for day 35: paclitaxel vs +CD95-Fc PLGA paclitaxel: *$P = 0.012$; day 35: paclitaxel vs −CD95-Fc PLGA paclitaxel: $P =$ ns; day 41: paclitaxel vs +CD95-Fc PLGA paclitaxel: *$P = 0.03$; day 41: paclitaxel vs −CD95-Fc PLGA paclitaxel: $P =$ ns; day 48: paclitaxel vs +CD95-Fc PLGA paclitaxel: **$P = 0.0093$; day 48: paclitaxel vs −CD95-Fc PLGA paclitaxel: *$P = 0.02$. (B), Imaging examples for the ovarian cancer bioluminescent xenograft study.

indicated in metastatic breast cancer treatment. However, paclitaxel chemotherapy is associated with off-target toxicities including neutropenia, leukopenia, anemia, alopecia, neuropathy, diarrhea, nausea, vomitting, fatigue and in the case of Cremophor based formulations allergic reactions that may require premedication with steroids or antihistamines [29]. Paclitaxel is also susceptible to the development of drug resistance in common with many other cytotoxics [30]. However, there are on-going efforts to improve the use of this cytotoxic ranging from novel nanomaterial reformulations [31—33] to synergistic co-therapy with oncolytic viruses [34] aimed at increasing efficacy whilst reducing toxic side-effects.

In the particular case of ovarian cancer, there is a shift away from intravenous (IV) chemotherapy towards localised intraperitoneal (IP) delivery of paclitaxel. This is due to clinical trials showing an extension in overall survival for patients receiving IP chemotherapy (65.6 months) compared to those on IV alone (49.7 months) [35]. This study led the National Cancer Institute in the USA to issue a clinical announcement on intraperitoneal chemotherapy for ovarian cancer recommending that 'after primary surgery, women with optimally debulked International Federation of Gynecology and Obstetrics (FIGO) stage III ovarian cancer should be counselled about the clinical benefit associated with IV and IP administration of chemotherapy'. The reduction in death risk for IP chemotherapy was also confirmed by a Cochrane review of eight randomised control trials [36]. However, the use of IP administration does result in catheter associated complications including toxicity and presents an additional level of technical complexity [35,37]. Separately, there is emerging evidence that lower and more regular dosage of paclitaxel in advanced ovarian cancer is beneficial [38].

Our studies using IP delivered CD95 modified paclitaxel-loaded microparticles have the potential to develop on these recent findings in ovarian cancer and improve on the major drawback to chemotherapy, systemic toxicity. The reported formulation removes the need for the toxic Cremophor EL and ethanol solvents. CD95 targeting concentrates the active ingredient at CD95L positive tumour cells and would be expected to reduce off-target toxicity. The relatively large 1.5 μm drug-loaded particles will be effectively confined to the peritoneum further reducing paclitaxel exposure at non-target sites such as the nervous system. However, any immune cell involvement including uptake by peritoneal macrophages or NK cells and any consequential safety implications would need to be determined in future studies. The biodegradable PLGA microparticle matrix can be tailored to deliver sustained daily doses of paclitaxel from days to weeks to improve drug activity and reduce the need for regular administration which can be a burden on hospital resources and inconvenient to the patient.

The ability to preferentially deliver into CD95L expressing tumour cells, and to get a better result from a standard dose of proven drug, makes this an attractive platform for improving the effectiveness to toxicity ratio of cytotoxic drugs. Finding new mechanisms to deliver relatively large drug-loaded microparticles to the interior of cancer cells is a counterapproach to the current trend focussing on nanoparticles for drug delivery. Nanoparticles still present unresolved issues around safety [20] but the real advantage of microparticles may be higher volume drug loading. Particles of one micron are about 125-fold the volume of their 200 nm counterparts, enabling more drug molecules to be packaged and better control over sustained payload release profiles. Targeting is in keeping with recent strategies for achieving specific delivery of therapeutics in cancer including genetically engineered cells [39], aptamer targeted nanoparticles [40] or CD22 targeted liposomes [41]. The use of CD95 represents an innovative ability to target therapeutics and exploit an often over-expressed ligand in cancer that normally promotes tumour growth [18,19] and facilitates immune-evasion [10].

5. Conclusions

Our findings suggest that CD95 modified microparticles are phagocytosed by CD95L expressing cells and that this mechanism is useful in drug delivery. Further studies are needed to shed light on this previously unrecognised function for the increasingly important CD95/CD95L system and elucidate the molecular pathways involved. This type of formulation could be applicable to many cancers, administered by direct intratumoural injections, as intracavity treatment or as an adjuvant following surgery to reduce the likelihood or viability of micrometastases, particularly since microparticles may be transported to loco-regional lymph nodes via natural lymphatic drainage channels. Newer biological drugs with intracellular targets including peptides, proteins and nucleic acids could also be incorporated into delivery particles raising the possibility of protected delivery of molecules not previously considered viable agents for development.

Conflict of interest

Davidson Ateh and Joanne Martin are Directors and shareholders of BioMoti Ltd (UK) that has rights to intellectual property associated with this work. Gert Veldhuis is Managing Director and shareholder of Nanomi BV (The Netherlands) that has rights to microsieve emulsification technology used in this work.

Acknowledgements

Appendix A. Supplementary material

Supplementary data associated with this article can be found, in the online version, at doi:10.1016/j.biomaterials.2011.07.060.

References

[1] Nagata S. Apoptosis by death factor. Cell 1997;88:355—65.
[2] Nagata S, Suda T. Fas and Fas ligand: lpr and gld mutations. Immunol Today 1995;16:39—43.
[3] (GNF) TGIotNRF. FAS (Fas (TNF receptor superfamily, member 6)). BioGPS gene annotation portal; 2011.
[4] (GNF) TGIotNRF. FASLG (Fas ligand (TNF superfamily, member 6)). BioGPS gene annotation portal; 2011.
[5] Choi C, Benveniste EN. Fas ligand/Fas system in the brain: regulator of immune and apoptotic responses. Brain Res Brain Res Rev 2004;44:65—81.
[6] Landau AM, Luk KC, Jones ML, Siegrist-Johnstone R, Young YK, Kouassi E, et al. Defective Fas expression exacerbates neurotoxicity in a model of Parkinson's disease. J Exp Med 2005;202:575—81.
[7] Ethell DW, Kinloch R, Green DR. Metalloproteinase shedding of Fas ligand regulates beta-amyloid neurotoxicity. Curr Biol 2002;12:1595—600.
[8] Ackery A, Robins S, Fehlings MG. Inhibition of Fas-mediated apoptosis through administration of soluble FAS receptor improves functional outcome and reduces posttraumatic axonal degeneration after acute spinal cord injury. J Neurotrauma 2006;23:604—16.
[9] O'Connell J, Houston A, Bennett MW, O'Sullivan GC, Shanahan F. Immune privilege or inflammation? Insights into the Fas ligand enigma. Nat Med 2001; 7:271—4.
[10] Ryan AE, Shanahan F, O'Connell J, Houston AM. Addressing the "Fas counterattack" controversy: blocking Fas ligand expression suppresses tumor immune evasion of colon cancer in vivo. Cancer Res 2005;65:9817—23.
[11] Igney FH, Krammer PH. Tumor counterattack: fact or fiction? Cancer Immunol Immunother 2005;54:1127—36.
[12] Green DR, Ferguson TA. The role of Fas ligand in immune privilege. Nat Rev Mol Cell Biol 2001;2:917—24.
[13] Gratas C, Tohma Y, Van Meir EG, Klein M, Tenan M, Ishii N, et al. Fas ligand expression in glioblastoma cell lines and primary astrocytic brain tumors. Brain Pathol 1997;7:863—9.

[14] Weller M, Schuster M, Pietsch T, Schabet M. CD95 ligand-induced apoptosis of human medulloblastoma cells. Cancer Lett 1998;128:121–6.

[15] Abrahams VM, Straszewski SL, Kamsteeg M, Hanczaruk B, Schwartz PE, Rutherford TJ, et al. Epithelial ovarian cancer cells secrete functional Fas ligand. Cancer Res 2003;63:5573–81.

[16] van Haaften-Day C, Russell P, Davies S, King NJ, Tattersall MH. Expression of Fas and FasL in human serous ovarian epithelial tumors. Hum Pathol 2003;34:74–9.

[17] Munakata S, Enomoto T, Tsujimoto M, Otsuki Y, Miwa H, Kanno H, et al. Expressions of Fas ligand and other apoptosis-related genes and their prognostic significance in epithelial ovarian neoplasms. Br J Cancer 2000;82:1446–52.

[18] Kleber S, Sancho-Martinez I, Wiestler B, Beisel A, Gieffers C, Hill O, et al. Yes and PI3K bind CD95 to signal invasion of glioblastoma. Cancer Cell 2008;13:235–48.

[19] Chen L, Park S-M, Tumanov AV, Hau A, Sawada K, Feig C, et al. CD95 promotes tumour growth. Nature 2010;465:492–6.

[20] Scheinberg DA, Villa CH, Escorcia FE, McDevitt MR. Conscripts of the infinite armada: systemic cancer therapy using nanomaterials. Nat Rev Clin Oncol 2010;7:266–76.

[21] Rabinovitch M. Professional and non-professional phagocytes: an introduction. Trends Cell Biol 1995;5:85–7.

[22] Bowen S, Ateh DD, Deinhardt K, Bird MM, Price KM, Baker CS, et al. The phagocytic capacity of neurones. Eur J Neurosci 2007;25:2947–55.

[23] Esselens C, Oorschot V, Baert V, Raemaekers T, Spittaels K, Serneels L, et al. Presenilin 1 mediates the turnover of telencephalin in hippocampal neurons via an autophagic degradative pathway. J Cell Biol 2004;166:1041–54.

[24] van Meerbergen B, Raemaekers T, Winters K, Braeken D, Bartic C, Spira M, et al. Improving neuronal adhesion on chip using a phagocytosis-like event. J Exp Nanosci 2007;2:101–14.

[25] Cohen S, Yoshioka T, Lucarelli M, Hwang LH, Langer R. Controlled delivery systems for proteins based on poly(lactic/glycolic acid) microspheres. Pharm Res 1991;8:713–20.

[26] Ryan AE, Lane S, Shanahan F, O'Connell J, Houston AM. Fas ligand expression in human and mouse cancer cell lines; a caveat on over-reliance on mRNA data. J Carcinog 2006;5:5.

[27] Veldhuis G, Gironès M, Bingham D. Monodisperse microspheres for parenteral drug delivery. Drug Del Technol 2009;9:24–31.

[28] Benard J, Da Silva J, De Blois MC, Boyer P, Duvillard P, Chiric E, et al. Characterization of a human ovarian adenocarcinoma line, IGROV1, in tissue culture and in nude mice. Cancer Res 1985;45:4970–9.

[29] Rowinsky EK, Donehower RC. Paclitaxel (taxol). N Engl J Med 1995;332:1004–14.

[30] Longley DB, Johnston PG. Molecular mechanisms of drug resistance. J Pathol 2005;205:275–92.

[31] Xiao K, Luo J, Fowler WL, Li Y, Lee JS, Xing L, et al. A self-assembling nanoparticle for paclitaxel delivery in ovarian cancer. Biomaterials 2009;30:6006–16.

[32] Yao HJ, Ju RJ, Wang XX, Zhang Y, Li RJ, Yu Y, et al. The antitumor efficacy of functional paclitaxel nanomicelles in treating resistant breast cancers by oral delivery. Biomaterials 2011;32:3285–302.

[33] Iqbal J, Sarti F, Perera G, Bernkop-Schnurch A. Development and in vivo evaluation of an oral drug delivery system for paclitaxel. Biomaterials 2011;32:170–5.

[34] Ingemarsdotter CK, Baird SK, Connell CM, Oberg D, Hallden G, McNeish IA. Low-dose paclitaxel synergizes with oncolytic adenoviruses via mitotic slippage and apoptosis in ovarian cancer. Oncogene 2010;29:6051–6.

[35] Armstrong DK, Bundy B, Wenzel L, Huang HQ, Baergen R, Lele S, et al. Intraperitoneal cisplatin and paclitaxel in ovarian cancer. N Engl J Med 2006;354:34–43.

[36] Jaaback K, Johnson N. Intraperitoneal chemotherapy for the initial management of primary epithelial ovarian cancer. Cochrane Database Syst Rev; 2006. CD005340.

[37] Bunting M, Chan W, Brand A, Blomfield P. Intraperitoneal chemotherapy for advanced epithelial ovarian malignancy: lessons learned. Aust N Z J Obstet Gynaecol 2009;49:667–71.

[38] Katsumata N, Yasuda M, Takahashi F, Isonishi S, Jobo T, Aoki D, et al. Dose-dense paclitaxel once a week in combination with carboplatin every 3 weeks for advanced ovarian cancer: a phase 3, open-label, randomised controlled trial. Lancet 2009;374:1331–8.

[39] Ma J, Reed KA, Gallo JM. Cells designed to deliver anticancer drugs by apoptosis. Cancer Res 2002;62:1382–7.

[40] Farokhzad OC, Cheng J, Teply BA, Sherifi I, Jon S, Kantoff PW, et al. Targeted nanoparticle-aptamer bioconjugates for cancer chemotherapy in vivo. Proc Natl Acad Sci U S A 2006;103:6315–20.

[41] Chen WC, Completo GC, Sigal DS, Crocker PR, Saven A, Paulson JC. In vivo targeting of B-cell lymphoma with glycan ligands of CD22. Blood 2010;115:4778–86.